

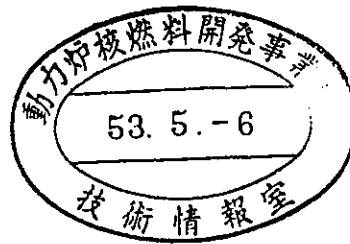
PNC TJS 250 75-14 Tr.

本資料はH13年11月30日付けで登録区分
変更する。

[技術情報グループ]

Sodium Oxide Aerosol Behavior in a Closed Chamber under Thermal Convection Flow

March 1978



Power Reactor and Nuclear Fuel Development Corporation

PNC T5250 75-14 Tr



Abstract

The present work was undertaken to obtain the effect of thermophoretic adherence of nuclear aerosol on the reactor containments in the event of a hypothetical accident of LMFBR. In the accident, sodium oxide aerosol containing PuO_2 - UO_2 fuel and fission products may be suspended in the containment and tends to deposit on the cold wall of the containment, so that the aerosol concentration decreases by thermophoresis in addition of settling and diffusional plating. Experiment was made to determine the relation for the degree of thermophoretic adherence of sodium oxide aerosol in a chamber. The results obtained by the experiment were compared with those of the calculation.

Sodium Oxide Aerosol Behavior in a Closed Chamber under Thermal Convection Flow.

1. Introduction

In the hypothetical accident of LMFBR, sodium oxide aerosol containing PuO_2 - UO_2 fuel and fission products may be suspended in the reactor containment. In this case, the temperature of gases in the primary containment rises rapidly, so that nuclear aerosol tends to deposit on cold wall of the containment by the thermophoresis due to the heating of sensible heat of the liquid sodium ejected from the reactor vessel, sodium combustion, and decay of fission products. On the other hand, the effect of settling will be hampered by soaring phenomenon of aerosol due to the thermal convection flow toward the ceiling of the containment. The number density of sodium oxide aerosol containing the fuel decreases to coagulation, settling, diffusional plating, and also due to thermophoretic deposition. Therefore, it is important to elucidate the thermal behavior of aerosol particles in safety of LMFBR at the hypothetical accident. The present work was carried out to obtain information on the thermophoretic deposition and soaring behavior of sodium oxide aerosol in a closed experimental chamber. Experiments were made to determine the relation between the degree of thermophoresis combined with the aerosol soaring and the heat transfer from hot gases to wall in the chamber. The results obtained by experiment were compared with those by calculation in rigid solution of the computer code (ABC-3) which was improved from the previous code¹⁾ and by approximation of ABC-3.

2. Theoretical treatment

2.1 Rigid solution

In the experiment, it is assumed that aerosol particles of sodium oxide (Na_2O) are dispersed in log-normal size distribution by the sodium combustion.

The aerosol will be stirred violently in the closed chamber, so that the radius of aerosol particles grows owing to the coagulation by Brownian motion. The aerosol of i th class particles agglomerated settles by gravitation according to the settling velocity $v_s(r_i)$ by the Stokes-Cunningham's equation. Small particles tend to deposit on the wall of chamber by the Brownian diffusion with the velocity of $v_d(r_i)$. Depending on the temperature of the chamber, small aerosol particles soar toward the ceiling and descend along the wall to bottom of the chamber in temperature gradient of $(T_g - T_w)/\delta_T$. The aerosol tends to adhere onto the cold wall due to thermophoresis. Assuming the radius of aerosol particles is in a continuum regime, i.e., $(\lambda/r) < 10$, the adhering velocity may be given by Brock's equation under influence of the temperature gradient, as follows²⁾:

$$v_T(r_i) = \frac{3\mu}{2\rho_a(273 + T_g)} \left[\frac{(k_g/k_p) + C_t(\lambda/r_i)}{\{1+3C_m(\lambda/r_i)\}\{1+2(k_g/k_p)+2C_t(\lambda/r_i)\}} \right] \left(\frac{T_g - T_w}{\delta_T} \right) \quad (1)$$

If thermal convection flow moves along the wall, the temperature gradient in the film sublayer on the wall is assumed in direction (y) perpendicular to the convection flow, as follows³⁾:

$$\frac{T_\infty - T}{T_\infty - T_w} = \left(1 - \frac{y}{\delta_T} \right)^2 \quad (2)$$

where, δ_T is the film thickness due to the convection flow, and T_∞ the temperature of gases outside the free stream. The heat transfer from hot gases to the wall is expressed as

$$Q = -k_g A \left(\frac{\partial T}{\partial y} \right)_{y=0} = \frac{2k_g A}{\delta_T} (T_g - T_w) = hA(T_g - T_w) \quad (3)$$

Therefore, the film thickness (δ_T) is given by the Nusselt's number for a free thermal convection under the turbulent flow ($10^{12} > Gr.Pr > 10^8$) as

$$\delta_T = \frac{2k_g}{h} = \frac{2H}{Nu} = \frac{2H}{0.129(Gr.Pr)^{1/3}} \quad (4)$$

where Gr and Pr are Grashof and Prandtl numbers, respectively. The value of v_T is obtained in substitution of δ_T into Eq.(1).

In the hypothetical accident of LMFBR, the basic equation for the k th class particles in the primary reactor containment is given as

$$\frac{dN_k}{dt} = \Gamma(t) - \left\{ \frac{v_s(r_k)}{H} + \frac{v_d(r_k)S}{V} + \frac{v_T(r_k)(S-S_F)}{V} - \frac{v_F}{H} \right\} N_k - \frac{L}{V} N_k + S_k(t) \quad (5)$$

$$\text{where } \Gamma(t) = \frac{1}{2} C_f \sum_{j=1}^{i=k-1} C_{ij} N_i N_j - C_f N_k \sum_{j=1}^{\infty} C_j N_j \quad (6)$$

and

$$C_f = \frac{2k(273 + T)}{3\mu}, \quad C_{ij} = (r_i + r_j) \left(\frac{r_i + A_i \lambda}{r_i} + \frac{r_j + A_j \lambda}{r_j} \right)$$

The term of $\Gamma(t)$ is the rate of production for the k th class particles and the disappearance rate of the same particles due to the coagulation, satisfying the relation of $v_k = v_i + v_j$ and $k = i + j$. The second to fourth terms represent removal effects of aerosol due to settling, wall plating, and thermophoresis, respectively. The fifth is the effect of soaring (v_F/H) for aerosol particles due to the ascending flow. The sixth is the effect of aerosol leakage from the primary containment. $S_k(t)$ is the source term of k th class aerosol particles.

The concentration of aerosol particles is obtained by summation of the number density, N_k , for the individual particles calculated from Eq.(5), using the ABC-code, as follows.

$$C(t) = \frac{4}{3} \pi \rho \sum_{i=1}^{\infty} r_i^3 N_i(t) \quad (7)$$

2.2 Approximate solution

To elucidate the thermal behavior of aerosol particles in the closed chamber, it is necessary to eliminate the complex term for particle coagulation $\Gamma(t)$, the leakage, and the source term $S_k(t)$. To remove the coagulation effect, the aerosol generation must be reduced considerably in the chamber. In this case, the effect of collision will be lowered due to the dilution of aerosol concentration, so that the particle size distribution will not vary largely with time; $\Gamma(t) = 0$ will be possible. Therefore, the logarithmic mean radius of aerosol particles (r_g) and logarithmic standard deviation (σ_g) may be constant with lapse of time due to the diluted aerosol concentration. Neglecting $\Gamma(t)$, leakage, and $S_k(t)$, the concentration decrease of aerosol is expressed from Eq.(5) as

$$\frac{C}{C_0} = \exp\left[-\left\{\frac{v_s(\bar{r})}{H} + \frac{v_d(\bar{r})S}{V} + \frac{v_T(\bar{r})(S-S_F)}{V} - \frac{v_F}{H}\right\} t\right] \quad (7)$$

where C_0 and C are the initial concentration in the chamber and the concentration at time t , respectively. $v_s(\bar{r})$, $v_d(\bar{r})$, and $v_T(\bar{r})$ are the average velocities of settling, plating, and thermophoresis, respectively:

$$v_s(\bar{r}) = \frac{2\rho g}{3\mu} \bar{r}^2 \left(1 + \frac{\bar{A} \lambda}{\bar{r}}\right) \quad (8)$$

$$v_d(\bar{r}) = \frac{\bar{D}}{\delta_d} = \frac{k(273+T)}{6\pi\mu\bar{r}\delta_d} \left(1 + \frac{\bar{A} \lambda}{\bar{r}}\right) \quad (9)$$

$$v_T(\bar{r}) = Z_T(\bar{r}) \left(\frac{T_g - T_w}{\delta_T}\right) \quad (10)$$

$Z_T(\bar{r})$ in Eq.(10) is a function of the thermophoresis by Brock for the average mean radius \bar{r} obtained from following equation, which is represented by r_g and σ_g in log-normal size distribution of the aerosol:

$$\bar{r} = r_g \exp(0.5 \ln^2 \sigma_g) \quad (11)$$

3. Experimental procedure

3.1 Apparatus

In the thermal behavior of aerosol particles in the closed chamber, it is necessary to have two different simulations of the flow, i.e., ideal and mixing, as shown in Figs.1 and 2. The closed chamber is 2 m high, with volume nearly 1 m^3 . Around the wall of chamber, a cooling coil is provided to obtain the temperature gradient between air and wall. The chamber is insulated perfectly by a glass wool mat: the heat generated in the chamber thus transfers completely to the cooling water through the wall. A specific amount of sodium is placed in a burnpot within the chamber: the sodium is heated in argon above 500°C and then ignited with air flow. At the center of the chamber, a heated chimney insulated with asbestos stands perpendicularly to obtain the ideal thermal convection. Therefore, the hot air containing sodium aerosol is emitted from the mouth of chimney, then flows down along the wall chamber; adhesion of the aerosol onto inner wall of the chimney is very small because of the thermal repulsive force acting on the aerosol. The temperature difference between circulating hot air and cold wall is measured continuously by thermocouples at the upper and the lower points, about 10 cm into the chamber wall and in contact with the cold wall, respectively. In Fig.2, the chamber is the same as in Fig.1; but the hot-plate heat source is placed as on the floor. Therefore, the convection of air occurs perpendicularly for the floor, and the aerosol settling in the chamber is hampered.

3.2 Methods

Before the experiments, electric current of the heat source is held constant for half a day, to obtain a steady temperature gradient in the two apparatuses, which increases with heating wattage of the heat source. In the experiment, sodium metal of 0.5 to 1.5 g is fired in the burnpot. The temperature difference is determined by the wattage, and the temperature of air rises about $2 - 4^\circ\text{C}$ due to

sodium combustion in the burnpot. The average temperature differences between the upper and lower in points are shown in Table 1. Sodium oxide aerosol in the chamber was taken by a particulate filter, and the concentration is determined by atomic absorption spectrophotometry. The size distribution of aerosol particles is determined by sampling with grids in a thermal precipitator, and plotted on a logarithmic-probability paper, counting particles on the grids with an electron microscope.

4. Results

4.1 The chimney-type heating

In the aerosol generation of high concentration, the radius of aerosol particles grows rapidly owing to coagulation, so that the gravitational settling is governed by the agglomeration of aerosol. However, if the dilute concentration of aerosol is used, the collision frequency of aerosol particles will be negligible, so that the variation of size distribution may be small in the chamber. The effect of thermophoresis is thus studied, in addition to the effects of settling and wall plating. The experiment by chimney-type heating was performed to obtain the ideal free thermal convection, as shown in Fig.1. The hot air flows out of the mouth of the chimney. Therefore, the setting is not hampered by the ascending flow of hot air except at the mouth, i.e., the settling occurs outside of the chimney because of the insulation by asbestos.

Fig.3 shows a plot of the concentration decrease of aerosol with lapse of time on semi-logarithmic paper; for the initial concentration of 5000 mg/m^3 in combustion of 15 g metallic sodium. The curves are not straight, which indicates that the coagulation due to high concentration is large, that is, the coagulation term of $\Gamma(t)$ in Eq.(5) cannot be neglected in the experiment. In the amount of heat flux which is expressed by the ratio of watt to area of the floor, the soaring

of aerosol appears above 4000 W/m^2 in spite of the insulation around the chimney. Fig.3 also shows the curves for the initial concentration of 1000 mg/m^3 in combustion of 5 g metallic sodium burnt; but the effect of coagulation still remains.

It is necessary to have dilute sodium oxide aerosol, to remove the complex phenomenon of coagulation. Fig.4 shows the concentration decrease with time in the case of dilute sodium oxide aerosol of initial concentration 70 mg/m^3 , with the heat flux up to 2900 W/m^2 . From the relation of straight line between concentration decrease and time, the effect of coagulation is seen to be negligible. Therefore, the aerosol concentration decrease in the closed chamber can be expressed by the approximate solution of Eq.(7). The concentration decrease of aerosol is enhanced in the heat flux, because of the strong thermophoresis of the aerosol. The concentration decrease without heating ($W/m^2 = 0$), to neglect the thermophoretic deposition onto the wall, is approximately as follows:

$$\frac{C}{C_0} = \exp\left[-\left\{\frac{v_s(\bar{r})}{H} + \frac{v_d(\bar{r})S}{V}\right\} t\right] \quad (12)$$

Therefore, the slope of straight lines without heating represents only the effects of settling and wall plating. In the heating experiment, the effect of thermophoresis is obtained from the difference between slopes with and without heating. Table 1 shows the results by calculation from Eq.(7) at $v_F = 0$ and those by the experiment. From the straight line in cumulative percentage of particles plotted on a logarithmic-probability paper in Fig.5, the size distribution of aerosol is found to be log-normal having $r_g = 0.16 \mu\text{m}$ and $\sigma_g = 2.0$.

The results by experiment and by calculation are in agreement in spite of the mean radius (\bar{r}) used in Eqs.(8)-(11). Therefore, the thermophoretic deposition under the ideal free thermal convection is thus confirmed by the calculation combin-

ing the Brock's equation and the Nusselt-type equation of free thermal convection. Fig.6 shows the average velocity (\bar{v}_T) of sodium oxide aerosol due to thermophoresis vs.the heat flux (W/m^2). The open and solid circles in figure were obtained by the calculation and experiment, respectively; the relation between \bar{v}_T and heat flux is nearly straight line.

Though the experimental results of the concentration decrease agree with the calculation by Eq.(7), it is necessary to confirm the calculation by code ABC-3 with the Eqs.(5)-(7). Table 2 shows the inputs for thermal behavior of the aerosol in the $1 m^3$ closed chamber. With the inputs, the results for initial concentration $70 mg/m^3$ are shown in Fig.7. The approximate solution of Eq.(7) is thus justified by the agreement with the values by ABC-3.

4.2 The hot-plate type heating

In the hypothetical accident, it is considered that sodium containing the fuel will spread flat on the floor by the ejection from the reactor vessel, causing a sodium fire in the primary reactor containment. The experimental results with the apparatus in Fig.2 are to be compared with those of the chimney-type heating under the same conditions. Fig.8 shows the concentration decrease of sodium oxide aerosol in the case of the hot-plate heating, for the initial concentration of $70 mg/m^3$ in the chamber. Due to the dilute dispersed sodium oxide aerosol, the curves of concentration decrease and time are straight. Fig.9 compares the concentration decrease with time for the chimney and for the hot-plate type apparatuses, for the heat flux of about $2000 W/m^2$. Concentration decrease of the chimney-type heating proceeds in settling, compared with the hot-plate heating. In the hot-plate heating, the slope of concentration decrease is small due to soaring of the aerosol particles by the ascending flow of hot air in the chimney. Therefore, the concentration decrease in the hot-plate heating is hampered greatly by soaring of

the aerosol expressed as a positive value of (v_F/H) in Eq.(7). The effect of soaring is introduced by subtraction of the slope of chimney-type heating from that of hot-plate type heating; this is, the effect is obtained by the relation between Eq.(7) and the equation (13).

$$\frac{C}{C_0} = \exp\left[-\left\{\frac{v_s(\bar{r})}{H} + \frac{v_d(\bar{r})S}{V} + \frac{v_T(\bar{r})(S-S_F)}{V}\right\} t\right] \quad (13)$$

The relation between the average soaring velocity of sodium oxide aerosol and the heat flux was obtained by experiment, as shown in Fig.10. The aerosol density of sodium oxide is smaller than that of the sodium oxide aerosol containing fuel material, so that the soaring value in the figure is conservative for LMFBR hypothetical accidents. In Fig.11, the agreement is satisfactory between the experiment and the calculation by the code using the soaring values.

5. Discussion

The present work was performed to obtain information on the thermophoretic deposition and the aerosol soaring in the hypothetical accident. The thermophoretic velocity of the aerosol is reduced by a half under the thermal convection from the value in the case of a forced flow. That is, the equation of natural free convection along the vertical plate is of a second order in the direction of convection flow (see Eq.(2)), i.e., the thickness of δ_T in Eq.(4) is twice larger than that in flow through a heat exchanger pipe⁴).

Thermal behavior of the aerosol in the LMFBR hypothetical accident was studied by van de Vate in RCN, measuring the concentration decrease of gold aerosol particles in a closed chamber which had a constant temperature gradient between hot air and cold wall. He described that the decrease of aerosol concentration is enhanced by heating at the center of the floor. But its decrease rate is lowered in hot-plate heating on the floor, because the settling is hampered by

the ascending flow due to the heat source^{5,6)}. He examined the phenomenon in the range of heat flux 0 - 200 W/m², but the heat fluxes at the sodium fire accident are much larger than 5 - 50 kW/m² in the primary containment of LMFBR. In the sodium fire, it is known that the settling velocity is hampered considerably by the soaring effect of aerosol. The average soaring velocity vs. heat flux (W/m²), Q, can be expressed empirically as:

$$v_F \text{ (cm/hr)} = 0.0225 Q^{1.33} \quad (14)$$

When the settling velocity of aerosol particle is balanced with the soaring velocity, the following equation is given by the relation of $v_s(\bar{r}) = v_F$ as

$$\bar{r} \text{ (cm)} = [2.36 \times 10^{-5} \mu Q^{1.33} / \rho g (1 + \frac{\bar{A} \lambda}{\bar{r}})]^{1/2} \quad (15)$$

Therefore, the radius of aerosol particles in the settling velocity balanced by the ascending velocity is almost proportional to square root of the heat flux. If the heat flux is assumed to be 15 kW/m² due to sodium fire and sensible heat of liquid sodium at the accident, the threshold soaring value of logarithmic mean radius (r_g) balanced by settling is calculated as $r_g = 9.86 \mu\text{m}$. Thus the soaring effect is important in the early stage of the accident, for the evaluation of a plutonium oxide aerosol release to be on the conservative for the hypothetical accident.

The computer codes have been made in several countries, i.e., HAA-3 in A.I.⁷⁾, PARISEKO-II in Karlsruhe⁸⁾, and ABC-2 in JAERI¹⁾, to calculate the aerosol behavior in the reactor containment at the hypothetical accident, but the codes do not take into consideration the soaring effect. The basic equation of aerosol behavior should include the soaring effect, for the plutonium oxide release at the reactor accident to be conservative.

Acknowledement

The authors wish to thank Mr.M.Miyauchi in JAERI for his assistance and Mr.O.Kawaguchi, Mr.K.Akagane in PNC for their helpful discussion in performance of the work. The authors would like to express their gratitude to Prof.Y.Takashima in the Tokyo Institute of Technology for his encouragement in performing the work.

Notations

- \bar{A} = Cunningham's correction of \bar{r} particles,
 C_0 = initial concentration of aerosol generated in the chamber (g/cm^3),
 C_m = numerical constant in thermal force derived by Brock, (= 1.0),
 C_t = numerical constant by Brock, (= 3.32),
 \bar{D} = diffusion coefficient of \bar{r} particles (cm^2/sec),
 H = height of the chamber (cm),
 h = heat transfer coefficient ($\text{cal/cm}^2 \text{sec}^\circ\text{C}$),
 k = Boltzman's constant ($\text{gcm}^2/\text{sec}^2\text{K}$),
 k_g = thermal conductivity of air ($\text{cal/cm sec}^\circ\text{C}$),
 k_p = thermal conductivity of aerosol particles ($\text{cal/cm sec}^\circ\text{C}$),
 L = leak rate of air (cm^3/sec),
 N_k = particle number density of kth class aerosol particles (particles/cm^3),
 S = surface area of the chamber (cm^2),
 S_F = area of the floor in the chamber (cm^2),
 V = volume of the chamber (cm^3),
 v_k = volume of aerosol for kth class particle (cm),
 ρ = density of aerosol particles (g/cm^3),
 ρ_a = density of air (g/cm^3),
 δ_d = film thickness due to the Brownian diffusion (cm),
 λ = mean free path of air (cm),
 μ = viscosity of air (g/cm sec).

References

- 1) Nishio, G., Kitani, S., and Takada, J.: Nucl. Eng. and Design, 34, 417 (1975).
- 2) Brock, J.R.: J. Colloid Sci. 17, 768 (1967).
- 3) Rohsenow, W.M., and Choi, H.Y.: Heat, Mass and Momentum Transfer, Prentice-Hall, Englewood Cliffs, New Jersey 153-163 (1961).
- 4) Nishio, G., Kitani, S., and Takahashi, K.: Ind. Eng. Chem., Process Des. Develop., 13, 408 (1974).
- 5) van de Vate, J.F.: RCN-174, (1972).
- 6) van de Vate, J.F.: RCN-74-050, (1974).
- 7) Koontz, R.L., Baumash, L., Greenfield, M.A. et al.: AI-AEC-12977, (1970)., Hubner, R.S., Vaughan, E.U. and Baumash, L.: AI-AEC-13038, (1973)., Gieseke, J.A. Behn, R.C., Chace, A.S. et al.: BMI-1932, (1975).
- 8) Jordan, H., Schikarski, W and Wild, H.: Actes du VII^o Congres Inter. Soci. Francaise de Radioprotection., VII-SFRP/24, 129, (Versailles, 28-31, mai, 1974).

Table 1. Comparison between experimental and calculational results under a chimney-type heating condition.

Condition Power flux (W/m ²) Temp. difference (°C)	Calculational values				Experimental values			
	Grashof No. (-)	Nusselt No. (-)	δ_T (cm)	$v_T(\bar{r})$ (cm/hr)	$v_T(S-S_F)/V$ (1/hr)	$v_T(\bar{r})$ (cm/hr)	$v_T(S-S_F)/V$ (1/hr)	Cal./Exp. (-)
0	2.12×10^9	1.55×10^9	2.7	0.38	0.0186	-	-	-
200	4.84×10^9	3.55×10^9	2.03	1.14	0.0542	1.17	0.0525	1.03
500	8.70×10^9	6.35×10^9	1.68	2.48	0.118	2.05	0.0920	1.28
1000	1.23×10^{10}	8.96×10^9	1.51	3.87	0.173	3.65	0.163	1.06
1500	1.70×10^{10}	1.25×10^{10}	1.34	6.03	0.287	4.07	0.194	1.48
2000	2.18×10^{10}	1.59×10^{10}	1.23	8.48	0.403	8.13	0.388	1.04
2900	2.63×10^{10}	1.92×10^{10}	1.19	11.02	0.530	7.35	0.328	1.62

Initial concentration of sodium oxide aerosol: 70 mg/m³, $\{v_s(\bar{r})/H + v_d(\bar{r})S/V\} = 0.074$ (1/hr) (at 0 W/m²)

Table 2 Input data for the concentration decrease of sodium oxide aerosol under the condition of thermophoretic adherence of the aerosol in the 1 m³ experimental chamber, for the code ABC-3.

height of the experimental chamber (cm)	H = 200
volume of the experimental chamber (cm ³)	V = 1 × 10 ⁶
inner surface area of the experimental chamber (cm ²)	S = 6.27 × 10 ⁴
density of sodium oxide aerosol (g/cm ³)	$\rho = 0.6$
thickness of δ_d due to the Brownian diffusion (cm)	$\delta_d = 0.1$
surface area of the floor in the chamber (cm ²)	$S_F = 1.5 \times 10^4$
thermal conductivity of sodium oxide aerosol (kcal/m hr ⁰ C)	$k_g = 0.0264$
initial concentration dispersed in the chamber (g/cm ³)	$C_0 = 1 \times 10^{-7}$
logarithmic standard deviation of aerosol	$\sigma_g = 1.90$
logarithmic mean radius of aerosol (cm)	$r_g = 1.6 \times 10^{-4}$

Caption

- Fig.1 Schematic of an experimental chamber for the chimney-type heating.
- Fig.2 Schematic of the experimental chamber for the hot-plate type heating.
- Fig.3 Concentration decrease of sodium oxide aerosol with lapse of time for the initial aerosol concentrations of 1000 and 5000 mg/m^3 dispersed in the chimney-type chamber.
- Fig.4 Concentration decrease of sodium oxide aerosol with lapse of time for the initial aerosol concentration of 70 mg/m^3 dispersed in the chimney-type chamber.
- Fig.5 Particle size distribution of sodium monoxide aerosol under the initial concentration of 70 mg/m^3 dispersed in the chamber.
- Fig.6 Adhering velocity of sodium oxide aerosol to the chamber wall due to thermophoresis, as a function of heat flux.
- Fig.7 Calculation of concentration decrease of the aerosol with time obtained by ABC-3 code for the initial aerosol concentration of 70 mg/m^3 dispersed in the chimney-type chamber.
- Fig.8 Concentration decrease of sodium oxide aerosol with time under the soaring condition for the initial concentration of 70 mg/m^3 dispersed in the hot-plate type heating chamber.
- Fig.9 Concentration decrease of aerosol with time for the differences of thermophoretic adherence between the chimney-type heating and the hot-plate type heating under the heat flux of 2000 W/m^2 .
- Fig.10 Soaring velocity of sodium oxide aerosol vs. heat flux in the hot-plate type chamber.
- Fig.11 Calculation of concentration decrease of sodium oxide aerosol with time under the soaring condition obtained by ABC-3 code, for the initial concentration of 70 mg/m^3 dispersed in the hot-plate type chamber.

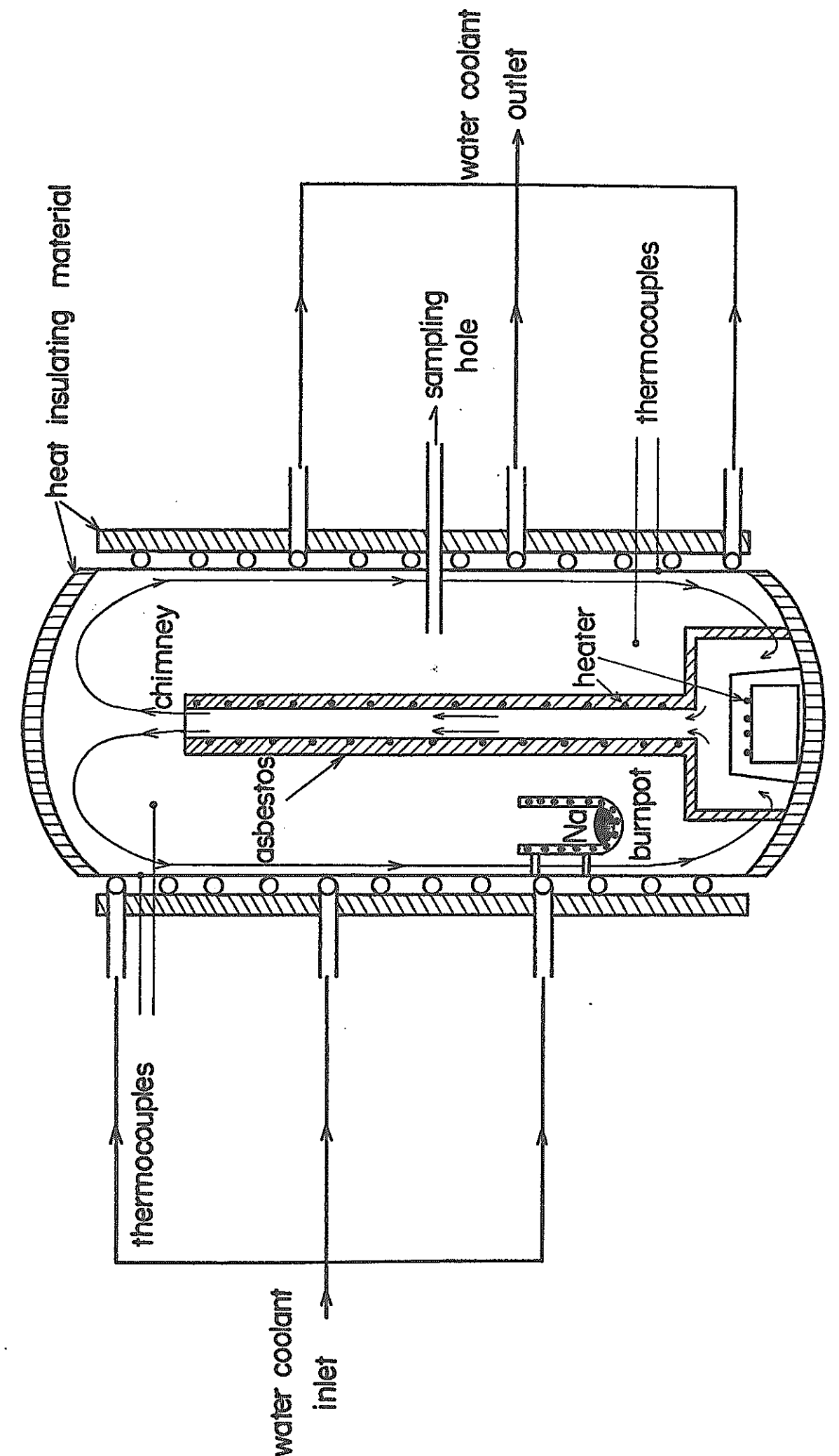


Fig. 1

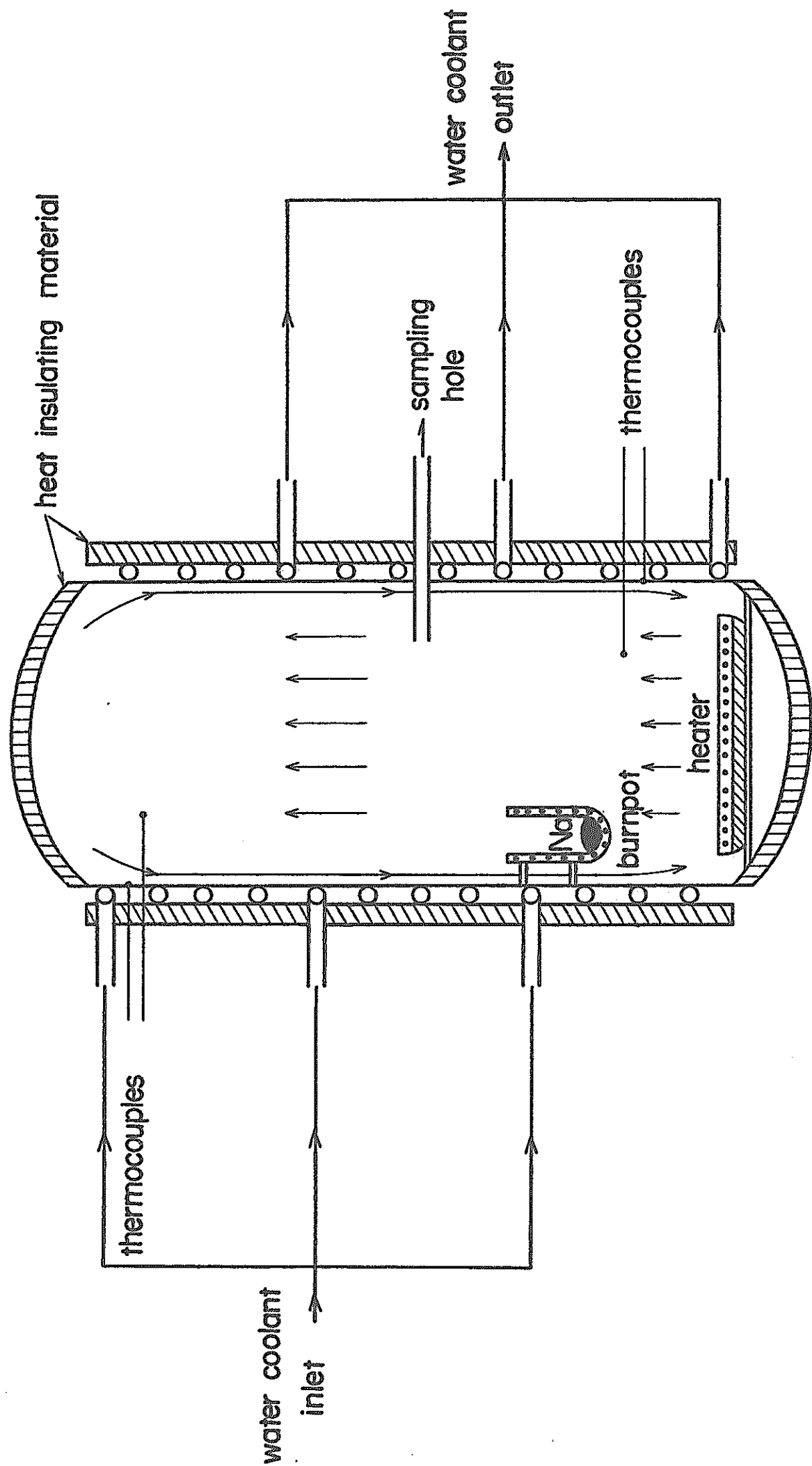


Fig. 2

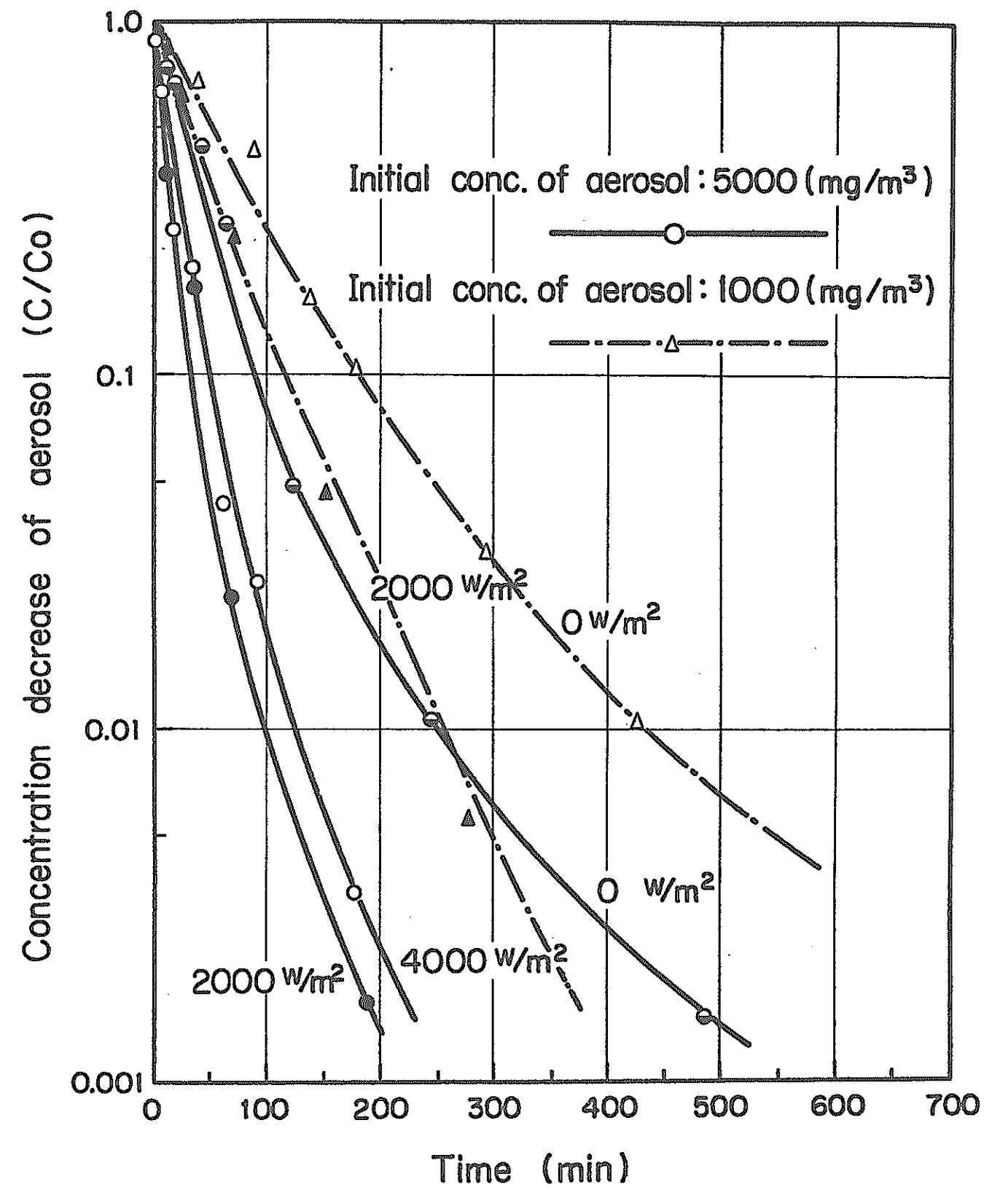


Fig. 3

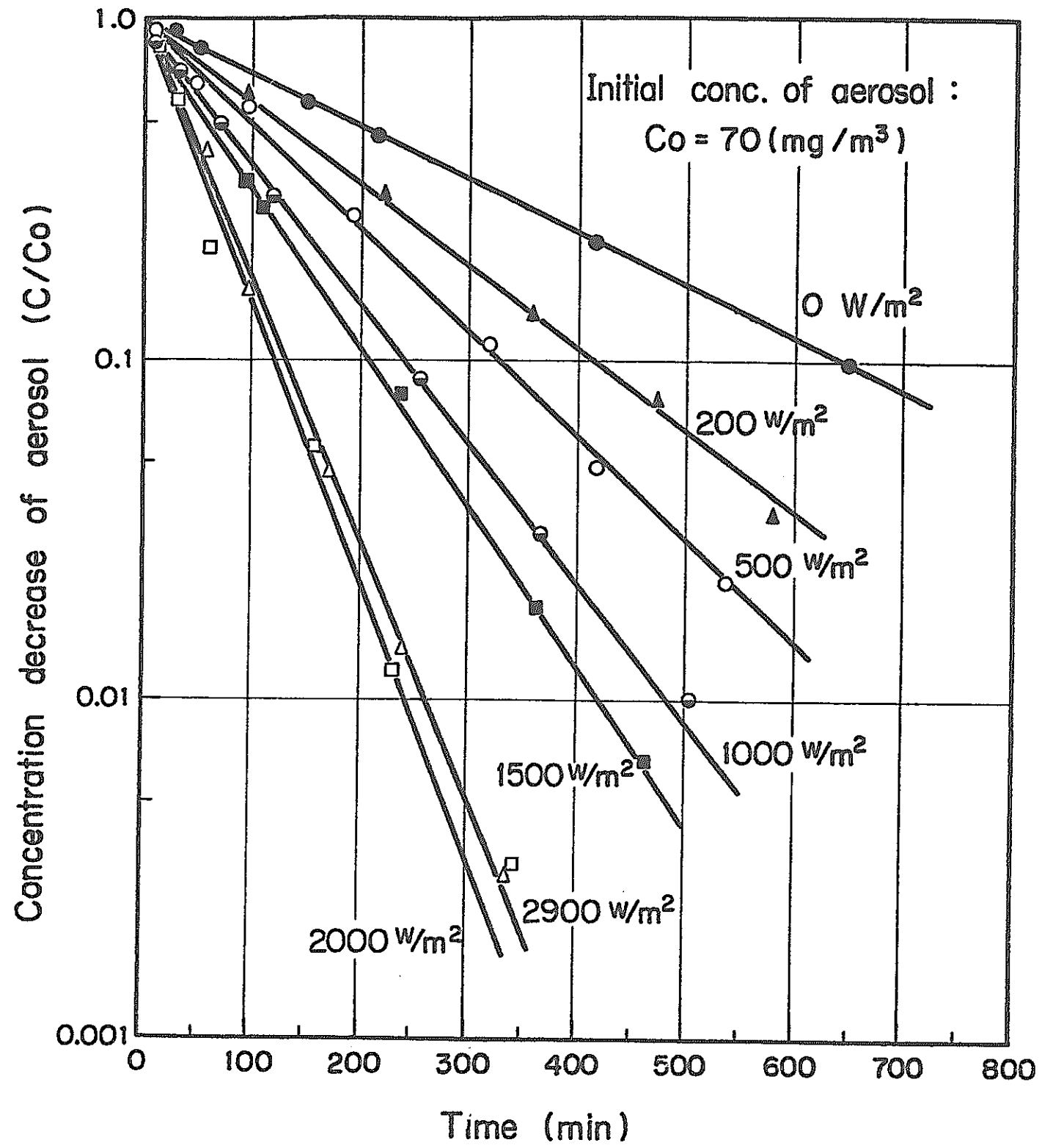


Fig. 4

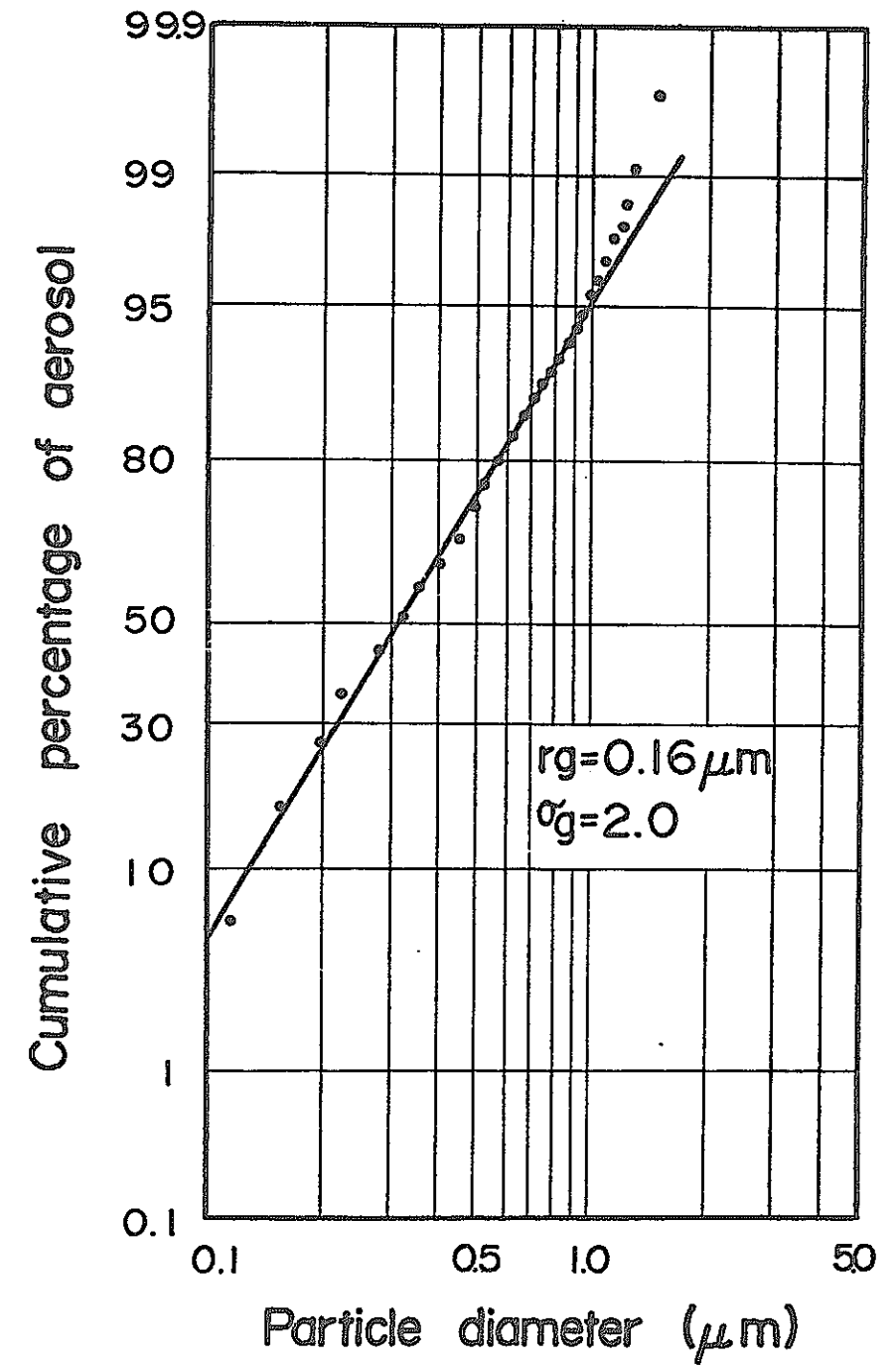


Fig. 5

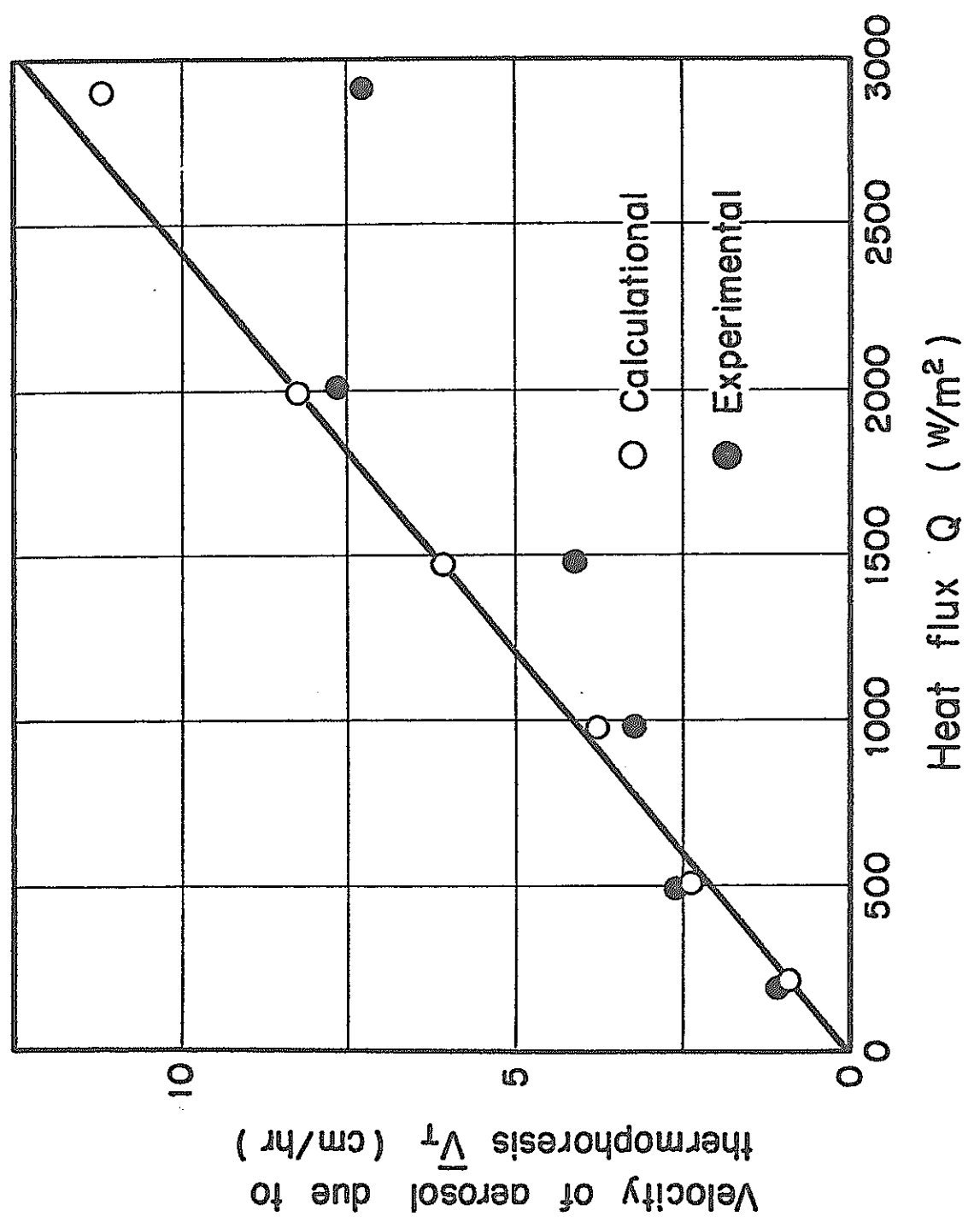


Fig. 6

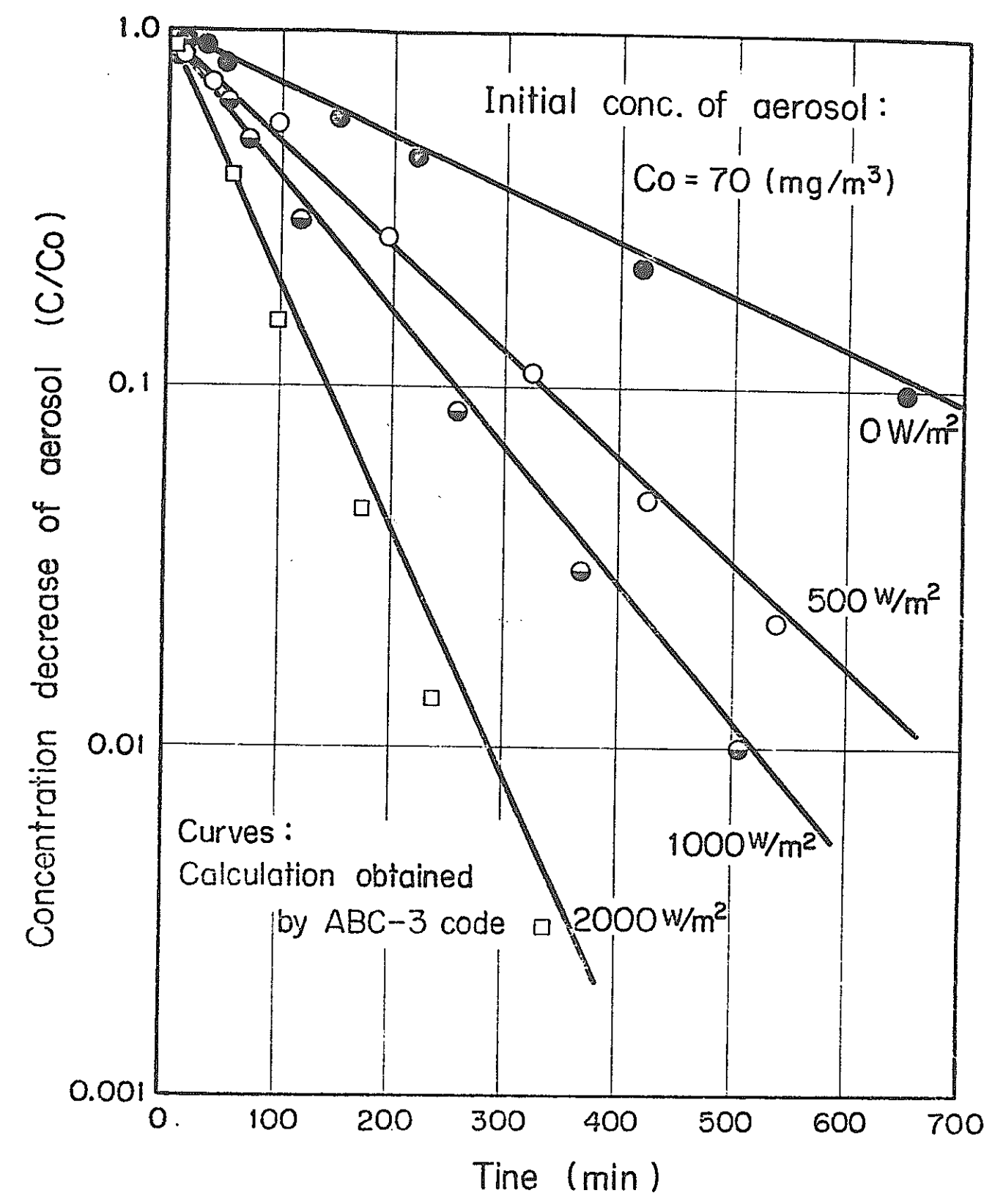


Fig. 7

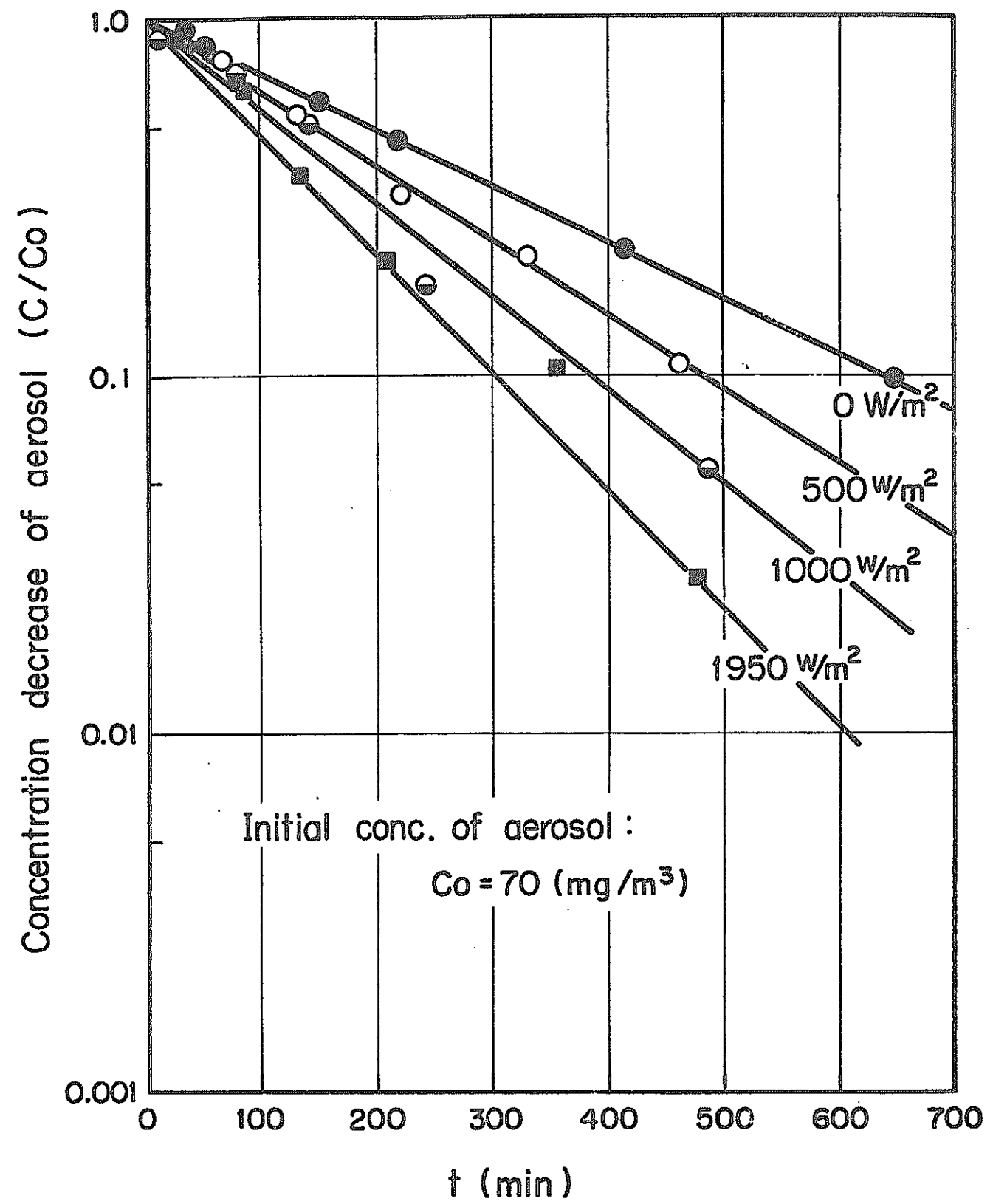


Fig. 8

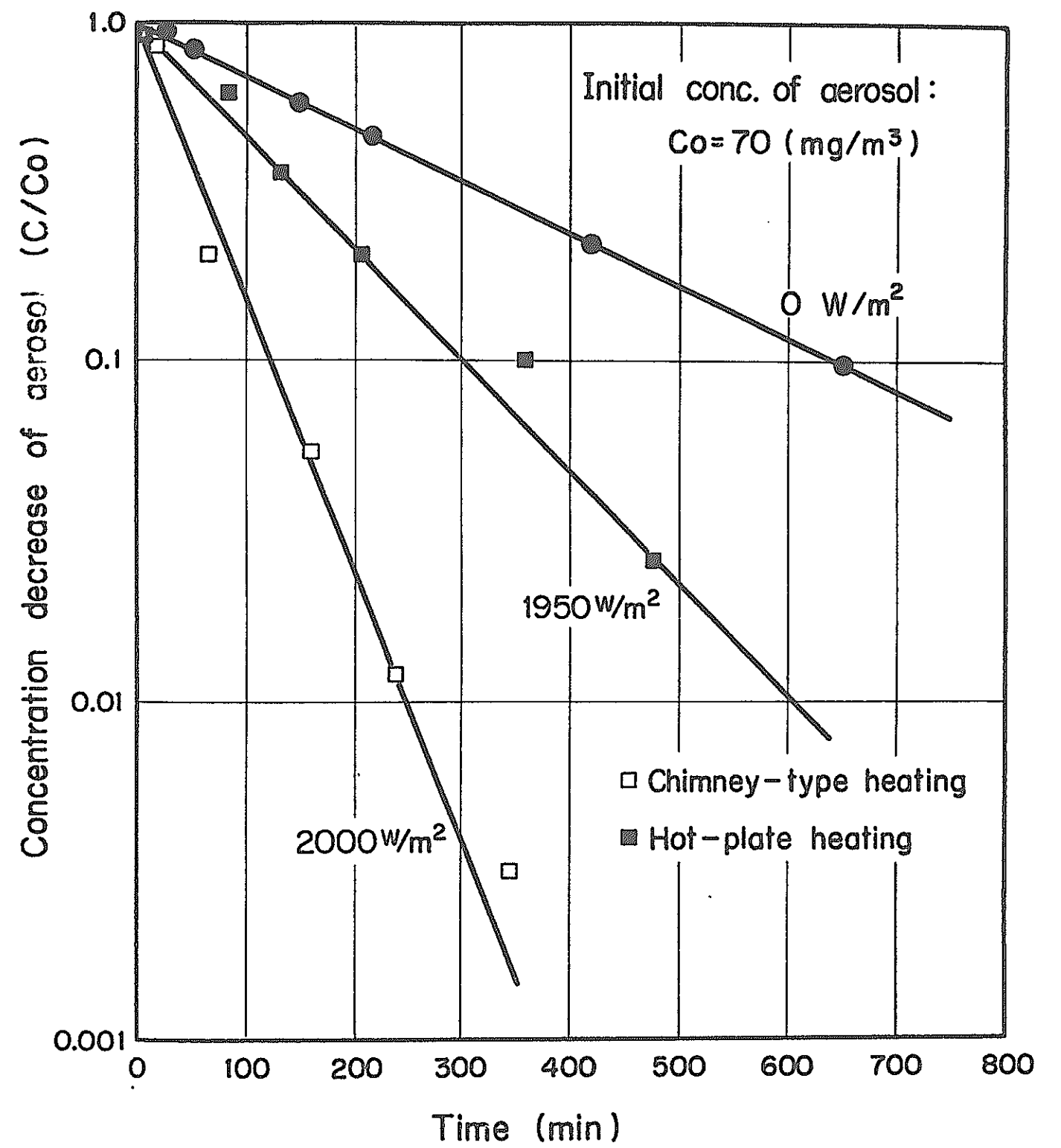


Fig. 9

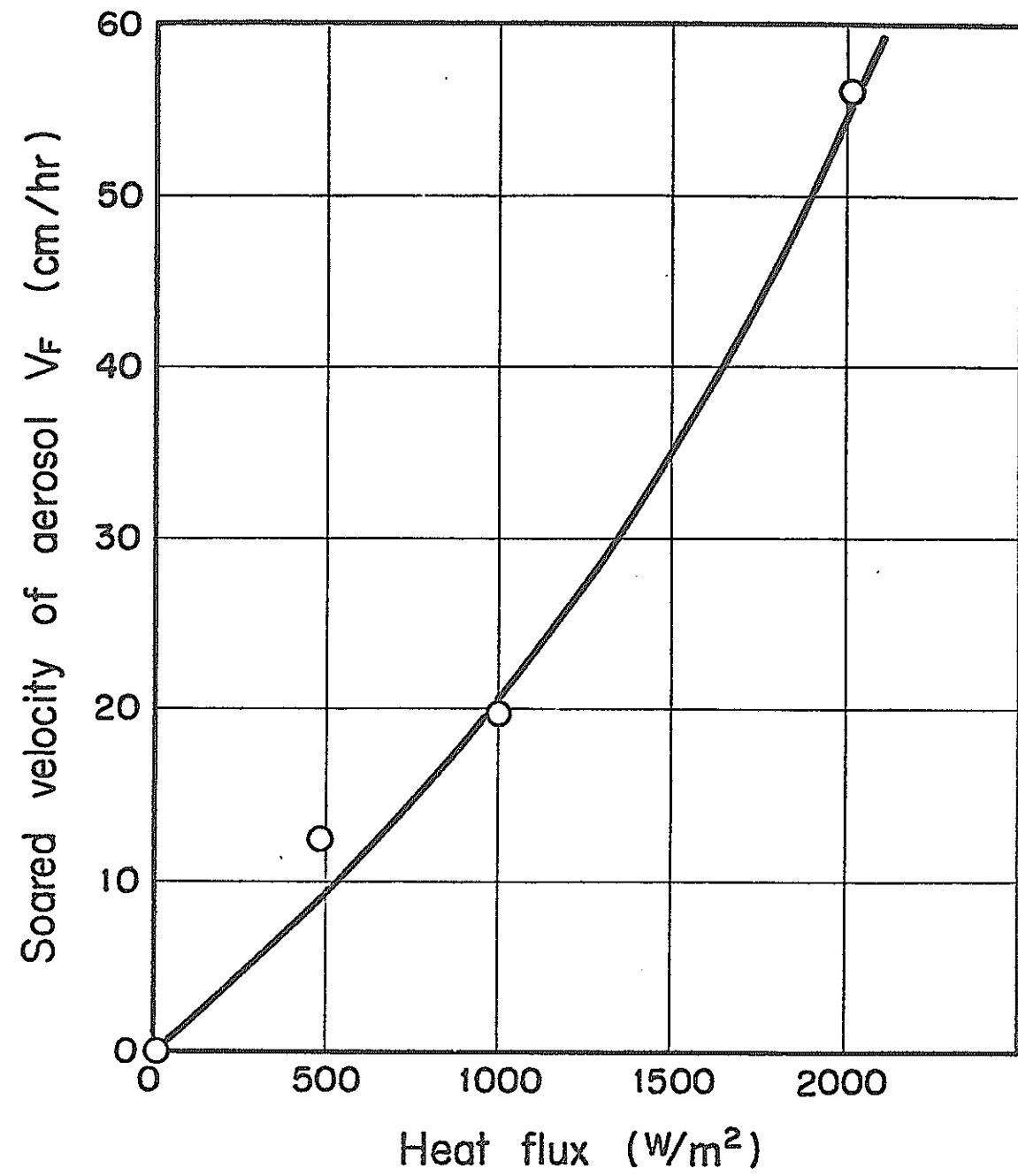


Fig. 10

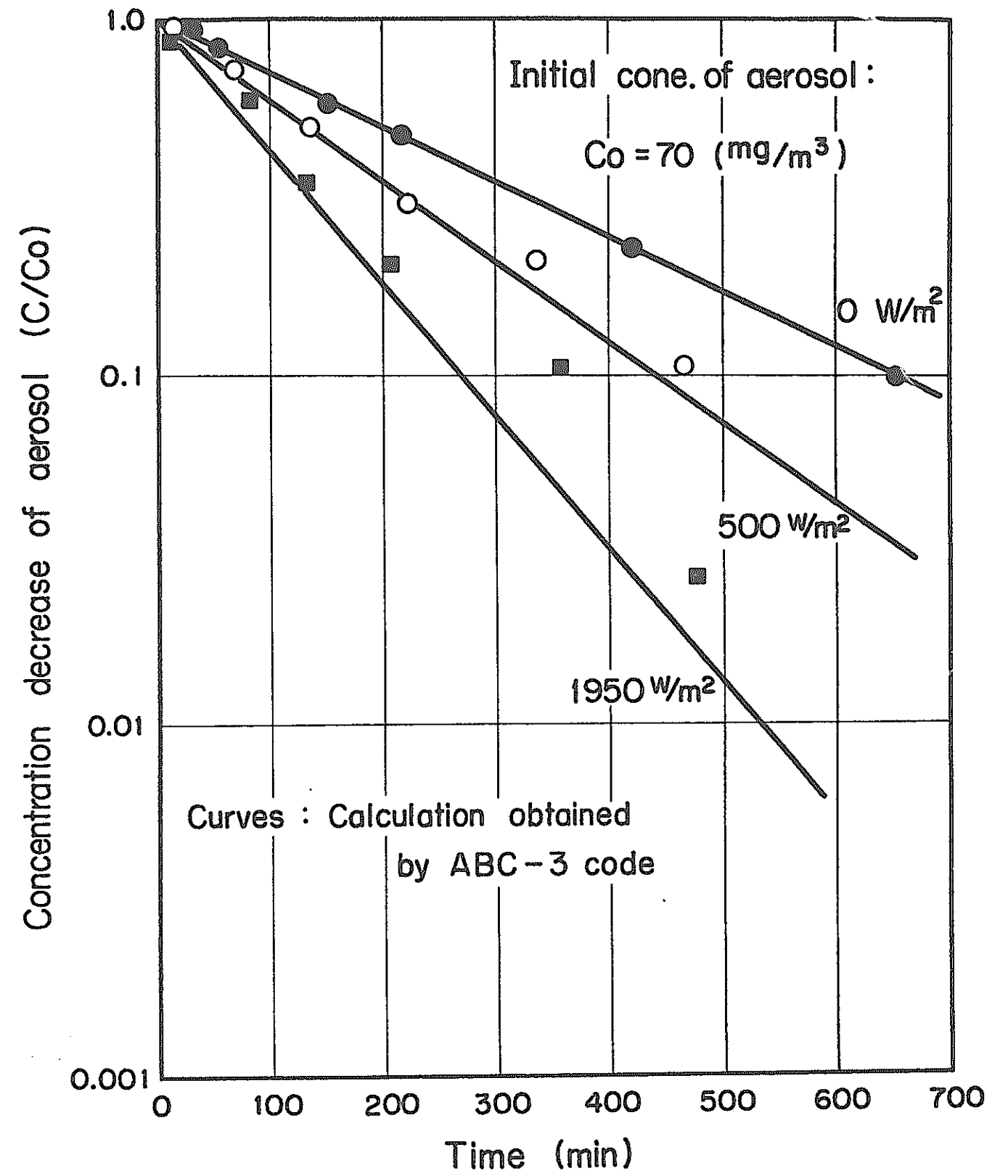


Fig. 11